International Journal of Computational Intelligence Systems
Vol. **14(1)**, 2021, *pp.* 965–977
DOI: https://doi.org/10.2991/ijcis.d.210216.001; ISSN: 1875-6891; eISSN: 1875-6883
https://www.atlantis-press.com/journals/ijcis/

Research Article

Slope Sliding Force Prediction via Belief Rule-Based Inferential Methodology

Jing Feng[1], Xiaobin Xu[1,*], Pan Liu[1], Feng Ma[2], Chengrong Ma[3], Zhigang Tao[4,5,*]

[1]*School of Automation, Hangzhou Dianzi University, Hangzhou, 310018, China*
[2]*Nanjing Smart Waterway Corp. Ltd, Nanjing, 210000, China*
[3]*College of Civil Engineering, Shaoxing University, Shaoxing, 312000, China*
[4]*State Key Laboratory for Geomechanics and Deep Underground Engineering, Beijing, 100083, China*
[5]*School of Mechanics and Civil Engineering, China University of Mining and Technology, Beijing, 100083, China*

ARTICLE INFO

Article History
Received 21 Sep 2020
Accepted 21 Jan 2021

Keywords
Slope landslide
Sliding force
Belief rule base
SLP optimization algorithm
West–East Gas Pipeline Project

ABSTRACT

Slope sliding force can be measured by an anchor cable sensor with the negative Poisson's ratio (NPR) property. It is capable of reflecting the stability of the slope intuitively. Thus, predicting the variation trend of the sliding force is able to achieve early warning for landslide disaster, thereby avoiding losses to the lives and property of the people. In this paper, due to the uncertain variation of the sliding force, a belief rule-based (BRB) sliding force prediction model is established to describe the nonlinear and uncertain relationship between the history/current sliding force and the future sliding force. In this model, the activated belief rules are fused by adopting the evidence reasoning (ER) algorithm. And based on the fused results, the sliding force at a future time can be predicted accurately. Moreover, considering the variation of the sliding force on different slopes or different monitoring points in the same slope, a parameter transfer strategy of BRB model together with a corresponding online update method are proposed to achieve the adaptive design of the BRB prediction model. Finally, the effectiveness of the proposed sliding force prediction methods has been verified by experiments on the sub-section of the China West–East Gas Pipeline Project.

1. INTRODUCTION

Slope landslides occur when sliding forces are greater than anti-sliding forces. It causes disasters, such as destroying railway and road traffic, damaging farmland and forests, destroying factories and mines, even drowning villages, which threaten people's lives and property. Normally, methods such as lidar technology [1], grating sensor technology [2], rainfall monitoring [3], groundwater level monitoring [4], are adopted to achieve early warning of slope landslides. However, these methods forecast landslides only by monitoring displacements and cracks [5], whereas the occurrence of the displacements and cracks does not necessarily cause landslides. Therefore, it is difficult for such methods to achieve accurate predictions.

Nevertheless, sliding forces are capable of reflecting the current state of the sliding body accurately. And the stability of slopes can be judged intuitively by measuring the sliding forces [6]. Thus, predicting the sliding forces is of great significance for early warning of disasters, so as to keep people's lives and property from damage. Moreover, research on predicting sliding forces is drawing more and more attention. Specifically, He *et al.* [7] developed a sliding force monitoring system based on a giant negative Poisson's ratio (NPR) anchor cable. In the system, a complex mechanical system is constructed by inserting a special artificial mechanical system into an unmeasured natural mechanical system [8, 9]. Bai *et al.* [10] used BP neural network to predict the slope stability of open-pit mine, and meanwhile pointed out that BP neural network is prone to fall into the local minimum. Li *et al.* [11] established a deformation and displacement prediction model of open-pit mine slope based on SVM, but the sensitivity of model parameters has not been further studied. Wang *et al.* [12] constructed a GM model-based on the Kalman filter to predict the deformation of highway slopes, but due to the complexity and mutability of highway slope deformation, the prediction accuracy was deficient. Sun *et al.* [13] proposed a monitoring and warning method of landslides in Pingzhuang West open-pit coal mine. The proposed method adopts the sliding remote monitoring and warning system which integrated the function of landslide reinforcement, detection, and warning, thereby realizing the whole process of slide force perception, transmission, analysis, monitoring, and warning. Tao *et al.* [14] adopt the plane polar projection method to analyze the landslide mechanism and use FLAC3D to build an NPR numerical analysis model which is used to make an early warning. However, the method cannot accurately grasp the magnitude of the sliding force at any time, and cannot be used for different slope migration and conversion.

*Corresponding author. Email: taozhigang@cumtb.edu.cn; xuxiaobin1980@hdu.edu.cn

At present, various sliding force monitoring and forecasting technologies have been successfully applied on 381 sites of 16 provinces across China, which involve slope monitoring on ancient landslides, high and steep loess natural slopes, urban construction slopes, open-pit coal mining, metal mining, highway project, and the West–East Gas Pipeline Project. Meanwhile, short-term and imminent warnings are able to be delivered after nearly ten years of sliding force monitoring and forecasting practice [15]. To be specific, early warning messages are successfully sent in all ten landslides, by which more than a hundred people's lives and hundreds of millions of property losses are saved [16]. However, by analyzing a large amount of engineering monitoring cases, it unveils that the existing sliding force prediction and early warning technologies may still be inadequate because of some inevitable problems:

- Due to the variation of regional climatic conditions and the disturbance of surroundings, sliding force monitoring is commonly affected by various uncertainty factors, thus the variation trend of sliding force may be unstable;
- As the sliding areas of each monitoring slope, the installation sites of NPR anchor cable and the construction conditions are various, the sliding force together with its features (e.g., changing range, dynamic change trend, etc.) which are collected at diverse monitoring points are different as well.

Overall, the above problems introduce difficulties constructing a universal slope sliding force prediction model, and also bring certain challenges to the further promotion of sliding force monitoring and early warning technology.

A belief rule-based (BRB) inferential methodology aims to describe uncertain data and knowledge. And it is capable of establishing complex nonlinear relationships between input and output variables [17–20]. Moreover, experts can construct belief rules and determine parameters based on their knowledge. Meanwhile, they are able to adjust model parameters by designing an optimization method based on historical data [21–23]. Obviously, the BRB inferential methodology integrates the advantages of data modeling and knowledge modeling, and has been applied perfectly in the field such as system performance prediction, safety assessment, fault diagnosis, and system identification [24, 25]. Moreover, the NPR anchor-based sliding force monitoring system holds the merit that the unmeasurable sliding force can be calculated from the measured data of the artificial mechanical.

In this paper, based on the above advantages, we propose a sliding force prediction model based on BRB inferential methodology. And sliding force monitoring on the sub-section of the West–East Gas Pipeline Project in China is taken as an example to verify the proposed method. Specifically, regarding the uncertainty problem of sliding force variation, an original BRB prediction model is constructed based on historical samples to describe the uncertainty and nonlinear relationship between input and output variables. For the self-adaptive adjustment of BRB models at different monitoring points, model parameter transfer and online optimization method are given to transplant the prediction model of the old monitoring point to the new monitoring point, so that the prediction of the sliding force at the new monitoring point is acquired accurately.

The structure of the paper is arranged as follows. The Section 2 describes the mathematical description of the sliding force prediction problem. By analyzing the sliding force monitoring data of the West–East Gas Pipeline Project, the input and output of the BRB model are determined. The Section 3 gives the construction method of BRB prediction model based on historical sliding force data. Section 4 illustrates transferring and online update of the BRB model. Section 5 demonstrates the process of initial BRB modeling, model transfer, and online update based on slope data of the West–East Gas Pipeline Project, which proves the effectiveness of the proposed method.

2. MATHEMATICAL DESCRIPTION OF THE SLIDING FORCE PREDICTION PROBLEM

2.1. Case Study of Sliding Force Monitoring

In this paper, the DD258 sub-section of the West–East Gas Pipeline Project is taken as an example and its slope topographic map is shown in Figure 1. In this case, sliding forces are collected from the NPR anchor cable sensors which are installed in the monitoring points, as shown in Figure 2. And the sliding forces are sampled every Δt seconds for totally $T\,(T >> 0)$ times with sampling time set as $t = 1, 2, \ldots, T$. For example, the sliding force at monitoring point *No.1* is collected every $\Delta t = 3h$ and 8 times a day from January to April 2008. And the variation trend of the sliding force at monitoring point *No.1* is shown in Figure 3. Seen from the figure, the curve can be divided into three sections, which are horizontal, ascending, and plunge. To be specific, Section AB is horizontal with small values and slow variations, which indicates that the slope is very stable. Sections BC, DE, and FG are ascending stages with increasing values but downward trends, with points C, E, and G as local peaks. Sections CD, EF, and GH are the stage of a sudden drop with sliding force values reaching the peak and decreasing sharply, which indicates that the structure of the landslide body at the monitoring point has changed. According to the experience of engineering applications, landslides usually occur 4 to 8 hours after the sudden drop stage.

Therefore, some conclusions can be drawn. Firstly, it is not necessary to predict Section AB as its values are relatively stable. Secondly, it is hard to predict Sections CD, EF, GH, due to their high uncertainty and variation. Thus, the mid-to-long-term prediction of sliding force in ascending Section BC is the primary concern. Therefore, by analyzing the variation trend of Section BC, an inference model is established to predict the variation of sliding force in the future, which is beneficial to make early warning for plunge phenomenon, so as to prepare protection measures in advance and further minimize the damage of casualties and property.

2.2. Mathematical Description of Sliding Force Prediction

In this paper, the sliding force of Section BC is set as $F_1 = \{f'(t) \,|\, t = 1, 2, \ldots, T\}$. Then the mathematical expression of the sliding force prediction problem is shown in Eq. (1), where $y(t+n)$ is the prediction of the sliding force at time $t+n$ in the future, $f'(t)$ is

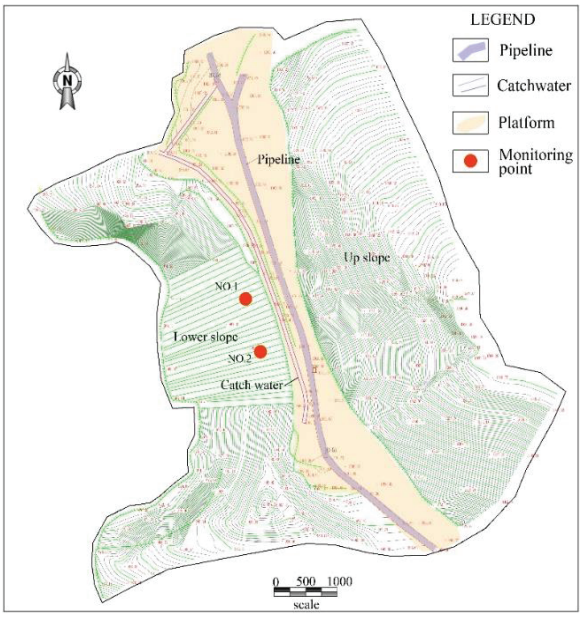

Figure 1 The slope topographic map of the DD258 sub-section of the West–East Gas Pipeline Project.

Figure 2 Sliding force monitoring points *No.1* and *No.2* on the slope.

the current observation at time $t, f'(t-1), f'(t-2), \ldots, f'(t-M)$ is M historical observations. And ψ is a constructed prediction model representing the relationship between observations and predictions in the future. In the model, the current observation at time t together with M historical observations are adopted to predict future sliding force at time $t+n$. As the time-varying trend of the sliding force is uncertain, it is difficult to construct the function ψ with a specific slope dynamics analytical model in reality. However, by obtaining a certain number of historical data, the prediction model can be constructed by data and knowledge-based methods. Certainly, the inputs of the model can also be some other variables relative to $f'(t), f'(t-1), f'(t-2), \ldots, f'(t-M)$ which are determined according to the real variation trend of $f'(t)$ case-by-case.

$$y(t+n) = \psi\left(f'(t), f'(t-1), \ldots, f'(t-M)\right) \quad (1)$$

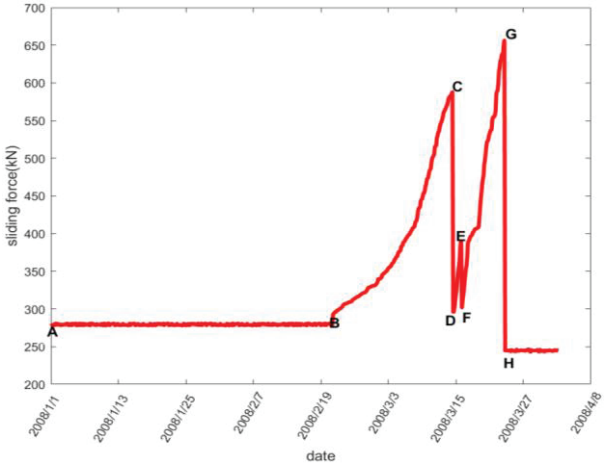

Figure 3 The variation trend of the sliding force at the monitoring point *No.1*.

Table 1 The list of variables and parameters of the belief rule-based (BRB) prediction model.

Variables	Explanation
A_i	The reference value of the i-th input variable
V_j	The reference value of the predicted sliding force $y(t+n)$
$\beta_{k,j}$	The belief degree of V_j in the k-th rule
θ_k	The relative importance of the k-th rule
δ_i	The relative importance of the input attribute $f_i(t)$
L	The number of rules
$\tilde{J}$	The number of clusters of the output vectors
$\tilde{L}_i$	The number of clusters of the i-th input variable
m_k	The time label of the minimum distance sample vector
w_k	The activated weight of the k-th rule
α_i^k	The matching degree of the i-th input variable and the reference value $A_{k,i} \in A_{i,1}, A_{i,2}, \ldots, A_{i,L_i}$ in the k-th rule
$D_{a,i}$	The interval width of the reference value of the i-th input variable
σ_1 and σ_2	Reduction factor
γ_I and γ_V	Enlargement factor
$\mu_{i,\tau}$ and φ_λ	Relative position ratio

3. THE BRB PREDICTION MODEL BASED ON HISTORICAL SLIDING FORCE

In the proposed model, BRB model is established to describe the nonlinear relationship between the historical/current sliding force and the future sliding force. In BRB model, the activated belief rules are fused by the evidence reasoning (ER) algorithm. Finally, the future sliding force can be calculated from the fused results. To better understand the model, the list of the variables is shown in Table 1.

3.1. The BRB-Based Sliding Force Prediction Model

The BRB system is an extension of the traditional IF–THEN rule expert system. It is capable of modeling and inferring incomplete, fuzzy, and uncertain data. And constructing belief rules is a key part of establishing a BRB system [26]. In a belief rule, each antecedent attribute has its corresponding reference value, and each consequent attribute corresponds to a belief distribution. As shown in the Eq. (2), the k-th rule is taken as an example, where $\theta_k\,(k=1,2,...,K)$ and K is the number of belief rules, $\delta_i\,(i=1,2,...,I)$ and I is the number of the antecedent attribute. Table 2 lists the physical interpretation of input and output variables and their related parameters in a BRB model.

$$\begin{aligned} R_k:\ &\text{If } f_1(t) \text{ is } A_{k,1} \wedge f_2(t) \text{ is } A_{k,2} \wedge ... \wedge f_I(t) \text{ is } A_{k,I} \\ &\text{Then } y(t+n) \text{ is } \left\{\left(V_1,\beta_{k,1}\right),\left(V_2,\beta_{k,2}\right),...,\left(V_J,\beta_{k,J}\right)\right\} \end{aligned} \tag{2}$$

Based on the above interpretation, the construction of the BRB sliding force prediction model and its inference process can be divided into the following steps:

(i) Confirm the input and output variables together with their reference values A_i and V_j.

(ii) Form the antecedent attributes of total $L_1 \times L_2 \times \ldots \times L_I$ rules by traversing every input reference value, and confirm the belief distribution of output reference value of each consequent attribute.

(iii) The input variable is adopted to activate rules of the BRB, and ER algorithm is adopted to fuse the belief distribution of the consequent attributes of the activated rules, from which $y\,(t+n)$ can be calculated.

In the following sections, a detailed analysis and introduction of the above steps are given.

3.2. Obtaining Input and Output Reference Values of BRB Based on Historical Data

Taking the case of monitoring point *No.1* shown in Figure 3 as an example, the sliding force in Section BC is used as historical data to confirm the input and output variables together with their reference values in the BRB model, respectively. According to the variation trend of the data in Section BC, the input variables are selected as in Eq. (3).

$$\begin{aligned} f_1(t) &= f'(t) \\ f_2(t) &= f'(t) - f'(t-1) \\ f_3(t) &= \left(f'(t) - f'(t-2)\right)/2 \end{aligned} \tag{3}$$

Concretely, compared with the sliding force observations obtained in single time $f'(t), f'(t-1), f'(t-2)$, the relative changes $f_2(t)$ and $f_3(t)$ are able to depict the subtle changes of the sliding force observations in adjacent time. Moreover, $f_1(t)$, $f_2(t)$, $f_3(t)$ and $y(t+n)$ in historical data are formed as a sample set $F_2 = \left\{\left(f_1(t), f_2(t), f_3(t), y(t+n)\right) | t=3,4,\ldots,T\right\}$, where the prediction $y(t+n)$ is equal to the true value $f_1(t+n)$ at the moment. And

Table 2 The physical interpretation of input and output variables of a belief rule-based (BRB) model.

The BRB System	The Physical Interpretation of Variables and Parameters
Antecedent attribute	Input variable $f(t) = \left(f_1(t),\ldots,f_I(t)\right)$
Reference value set $A_i = \left\{A_{i,l} \mid l=1,\ldots,L_i; i=1,\ldots,I\right\}$	The reference value of the i-th input variable A_i
The number of reference values of antecedent attributes L_i	L_i is the number of parameter values of the i-th input variable
The antecedent of the k-th rule, $k=1,\ldots,K$	Reference values of $f(t)$ in the k-th rule $A_k = \left(A_{k,1},A_{k,2},\ldots,A_{k,I}\right), A_{k,i} \in A_i$
The consequent of the k-th rule $\left\{\left(V_1,\beta_{k,1}\right),\ldots,\left(V_J,\beta_{k,J}\right)\right\}$,	$V_j\,(j=1,\ldots,J)$ is the reference value of the prediction of sliding force $y(t+n)$, $\beta_{k,j}$ is the belief degree of V_j
Number of conclude attributes J	J is the number of output variable parameter values
Rule weight $\theta_k \in [0,1]$	The relative importance of the k-th rule
Attribute weight $\delta_i \in [0,1]$	The relative importance of input attribute $f_i(t)$

F_2 can be broken up into four subsets: $X_1 = \left\{f_1(t) \mid t=3,4,\ldots,T\right\}$, $X_2 = \left\{f_2(t) \mid t=3,4,\ldots,T\right\}$, $X_3 = \left\{f_3(t) \mid t=3,4,\ldots,T\right.$, $Y = \left.\left\{y(t+n) \mid t=3,4,\ldots,T\right\}\right.$.

To avoid the randomness and subjectivity of the initial parameters of the model caused by the reference value given by the expert experience, K-means is adopted to cluster the subsets into K groups so that the selected reference value is in line with the change of the samples, thus, a better fusion calculation can be obtained. Specifically, K-means clustering is implemented on the subsets $X_i\,(i=1,2,3)$, with the cluster centers set as

$$\begin{aligned} &A_i = \left\{A_{i,1}, A_{i,2}, ..., A_{i,L_i}\right\}, \\ &\text{with } A_{i,1} < A_{i,2} < ... < A_{i,\tilde{L}_i} < A_{i,\tilde{L}_i+1} < A_{i,\tilde{L}_i+2}, \\ &\qquad A_{i,1} = \min_t\left\{f_i(t)\right\}, A_{i,\tilde{L}_i+2} = \max_t\left\{f_i(t)\right\} \end{aligned}$$

here $\tilde{L}_i\left(\tilde{L}_i \geq 1\right)$ is the number of cluster centers of the i-th input variable. The input reference values can be obtained as $A_i = \left\{A_{i,1}, A_{i,2}, ..., A_{i,L_i}\right\}$, where $i=1,2,3$, $L_i = \tilde{L}_i + 2$. Similarly, K-means is implemented on the set Y and the output reference values can be obtained as $V = \left\{V_1, V_2, ..., V_J\right\}$, $J = \tilde{J} + 2$, where $\tilde{J}$ is the number of cluster centers of the output variable.

3.3. Constructing BRB Based on Historical Data

After the input and output reference values are confirmed, the belief rules $L_1 \times L_2 \times \ldots \times L_I$ are constructed to form a BRB. Then $\beta_{k,j}$, the belief degree of the consequent attribute in each rule, needs to be confirmed. Here, $F_3 = \left\{\left(f_1(t), f_2(t), f_3(t)\right) | t=3,4,\ldots,T\right\}$ is set as the historical data of the input variables, and $\beta_{k,j}$ can be obtained by matching the data and the reference value of the antecedent

attribute in F_3. To be specific, firstly, Euclidean distance between the data in F_3 and the reference values of the k-th rule which are marked as $\left(A_{k,1}, A_{k,2}, A_{k,3}\right)$ can be calculated by Eq. (4), where $d_{m_k,k}$ is the minimum distance, m_k, $m_k \in \{3, 4, ..., T\}$ is the time label of the data with the minimum distance, specifically, it is the corresponding historical samples to the minimum distance.

$$\begin{aligned} d_{t,k} &= \sqrt{\sum_{i=1}^{3} \left(f_i(t) - A_{k,i}\right)^2}, i = 1, 2, 3; k = 1, 2, \ldots, K \\ d_{m_k,k} &= \min_t \left\{d_{t,k}\right\} \end{aligned} \tag{4}$$

After matching with $\left(A_{k,1}, A_{k,2}, A_{k,3}\right)$ in each rule, the most similar historical data samples of all rules can be obtained with the corresponding time label $S = \left\{m_1, m_2, \ldots, m_K\right\}$, then the historical data samples of the corresponding output variable $Y' = \left\{y'\left(m_k + n\right) | m_k \in \{3, 4, \ldots, T\}\right\}$ can be obtained. Finally, by calculating the matching degree of $y'\left(m_k + n\right)$ and the reference value of the consequent attribute in the k-th rule by Eq. (5), the corresponding $\beta_{k,j}, j = 1, 2, \ldots, J$ can be obtained.

$$\begin{cases} \beta_{k,j} = \frac{V_{j+1} - y'(m_k+n)}{V_{j+1} - V_j}, \beta_{k,j+1} = \frac{y'(m_k+n) - V_j}{V_{j+1} - V_j} & V_j \le y'\left(m_k + n\right) \le V_{j+1} \\ \beta_{k,1} = 1;\ \beta_{k,j} = 0\ \ (j \ne 1) & y'\left(m_k + n\right) < V_1 \\ \beta_{k,J} = 1;\ \beta_{k,j} = 0\ \ (j \ne J) & y'\left(m_k + n\right) > V_J \end{cases} \tag{5}$$

3.4. Obtaining Predicted Sliding Force Based on ER Algorithm

In the constructed BRB, the activated weight w_k of the input variables $\left(f_1(t), f_2(t), f_3(t)\right)$ regards to the k-th rule can be obtained from Eq. (6).

$$w_k = \theta_k \prod_{i=1}^{3} \left(\alpha_i^k\right)^{\overline{\delta_i}} / \sum_{k=1}^{K} \theta_k \prod_{i=1}^{3} \left(\alpha_i^k\right)^{\overline{\delta_i}} \tag{6}$$

Here, θ_k is the weight of the k-th rule, and the attribute weight is shown in Eq. (7).

$$\overline{\delta_i} = \delta_i / \max_{i=1,2,3} \left\{\delta_i\right\} \tag{7}$$

α_i^k is the matching degree of the i-th input variable $f_i(t)$ and the reference values $A_{k,i} \in \left\{A_{i,1}, A_{i,2}, ..., A_{i,L_i}\right\}$ in the k-th rule, which can be calculated from Eq. (5) by replacing V_J with $A_{k,i}$, $y'\left(m_k + n\right)$ with $f_i(t)$.

After the activated rule weights have been fixed, ER algorithm is adopted to fuse the belief distribution of consequent attribute with a different activated degree, so as to obtain the corresponding output of the input $\left(f_1(t), f_2(t), f_3(t)\right)$, as shown in Eq. (8).

$$\left\{\left(V_j, \beta_j\right) | j = 1, 2, ..., J\right\} \tag{8}$$

where β_j, which can be calculated by Eqs. (9) and (10), is the belief degree of the output reference value V_j.

$$\beta_j = \frac{\eta\left[\prod_{k=1}^{K}\left(w_k\beta_{k,j} + 1 - w_k \sum_{j=1}^{J}\beta_{k,j}\right) - \prod_{k=1}^{K}\left(1 - w_k \sum_{j=1}^{J}\beta_{k,j}\right)\right]}{1 - \eta\left[\prod_{k=1}^{K}\left(1 - w_k\right)\right]} \tag{9}$$

$$\eta = \left[\sum_{j=1}^{J}\prod_{k=1}^{K}\left(w_k\beta_{k,j} + 1 - w_k \sum_{j=1}^{J}\beta_{k,j}\right) - (J-1)\prod_{k=1}^{K}\left(1 - w_k \sum_{j=1}^{J}\beta_{k,j}\right)\right]^{-1} \tag{10}$$

Finally, the predicted sliding force $y(t+n)$ is obtained by a weight average operator as shown in Eq. (11).

$$y(t+n) = \sum_{j=1}^{J} V_j\beta_j \tag{11}$$

4. BRB MODEL TRANSFER AND ONLINE UPDATE STRATEGY

In this paper, the BRB sliding force prediction model at monitoring point *No.1* is denoted as BRB_a. It aims to use BRB_a to predict sliding force on other slopes or adjacent monitoring points with similar geological conditions. As shown in Figure 2, monitoring point *No.2* is adjacent to monitoring point *No.1* and the BRB sliding force prediction model at monitoring point *No.2* is represented as BRB_b with the sliding force curve shown in Figure 4. By comparing Section BC in Figure 3 and Section B′C′ in Figure 4, it can be concluded that although the monitoring points *No.1* and *No.2* belong to the same slope, the trends of their sliding force are different when the sign of landslide occurs. To be specific, (1) The benchmarks of sliding force at point *No.1* and *No.2* under a steady-state in Section AB and A′B′ are different, with the point *No.1* is 278.5 kN and the point *No.2* is 376.5 kN; (2) The duration and trend of Section BC and B′C′ are different, with the point *No.1* rises to the maximum value of 588.95 kN after 486 hours, and point *No.2* rises to the maximum value of 963 kN after 738 hours; (3) The sliding force variation ranges of Section BC and B′C′ are different. The variation ranges of monitoring point *No.1* and monitoring point *No.2* are 310.4 kN and 586.5 kN, respectively. In short, apart from the fact that the sliding force obtained at two different NPR sensor monitoring points has experienced a similar ascent process in Section BC, the other specific change characteristics are different. Therefore, BRB_a cannot be directly used to predict the sliding force at point *No.2*. It is necessary to adjust the parameters of the model BRB_a (parameter transfer) based on the data in the initial stage at point *No.2* (the data observed around monitoring time B′ in Figure 4). And then Sequential linear programming (SLP) online optimization is implemented on data acquired online so as to make BRB_a gradually adapt to the prediction of sliding force in Section B′C′ at the point *No.2*.

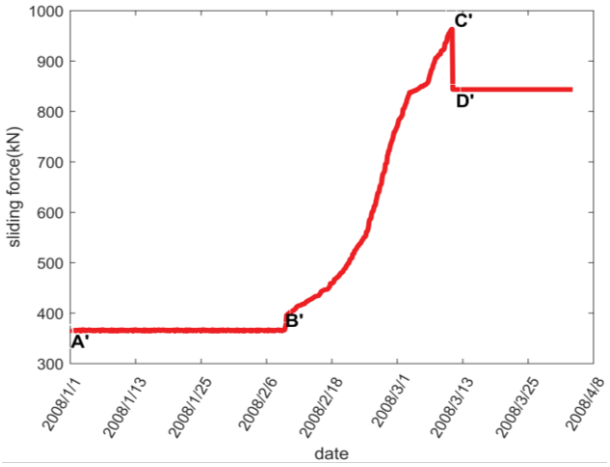

Figure 4 The variation trend of the sliding force at the monitoring point *No.2*.

4.1. Parameter Transfer of BRB Sliding Force Prediction Model for New Monitoring Point

The transferring of input and output reference values in the BRB model is actually to transplant the change law of the reference value in BRB_a to BRB_b. Thus, the position law of the reference value in BRB_a is calculated, and then the reference values can be transferred after the abnormal variation of the sliding force at point *No.2* is detected. The details are shown in the following three steps:

Step 1: Calculate the relative position ratio of the input and output reference values in BRB_a.

Firstly, the interval width of the input and output reference values in BRB_a can be obtained from Eq. (12), where $D_{a,i}$ is the interval width of the i-th input reference value, $D_{a,4}$ is the interval width of the output reference values.

$$D_{a,i} = A_{i,L_i} - A_{i,1}, D_{a,4} = V_J - V_1 \tag{12}$$

Secondly, the relative position ratio $\mu_{i,\tau}$ and φ_λ can be calculated from Eq. (13), where $\mu_{i,\tau}$ is the relative position ratio of the clustering center $A_{i,\tau}\left(\tau = 2, 3, ..., \tilde{L}_i + 1\right)$ of the input variable and the interval width $D_{a,i}$. φ_λ is the relative position ratio of the clustering center $V_\lambda\left(\lambda = 2, 3, ..., \tilde{J} + 1\right)$ of the output variable and the interval width $D_{a,4}$.

$$\mu_{i,\tau} = \left(A_{i,\tau} - A_{i,1}\right)/D_{a,i}, \varphi_\lambda = \left(V_\lambda - V_1\right)/D_{a,4} \tag{13}$$

Step 2: Determine the minimum and maximum of the input and output reference values in BRB_b.

Specifically, the input and output of BRB_b are denoted as $f_1^b(t), f_2^b(t), f_3^b(t)$ and $y^b(t+n)$, respectively. Obviously, the range of these variables needs to be determined in order to construct BRB_b. Seen from Figure 4, sliding force shows a significant increase at B'. And its value, which can be determined by the overrun detection method, is set as the minimum reference value of $f_1^b(t)$ and $y^b(t+n)$, and meanwhile marked as $A_{1,1}^b$ and V_1^b respectively. Then, two sliding force values after point B' are collected to acquire the initial values of $f_2^b(t)$ and $f_3^b(t)$ by Eq. (3), which are marked as $IV_{2,1}^b$ and $IV_{3,1}^b$, respectively. Further, the minimum reference value of $f_2^b(t)$ and $f_3^b(t)$ can be acquired by Eq. (14), where σ_1 and σ_2 are reduction factor which can be determined by experts so as to make $f_2^b(t)$ and $f_3^b(t)$ no small than $A_{2,1}^b$ and $A_{1,1}^b$. Next, the maximum value of the input and output can be obtained as shown in Eq. (15).

$$A_{2,1}^b = \sigma_1 IV_{1,1}^b, A_{3,1}^b = \sigma_2 IV_{3,1}^b \tag{14}$$

$$\begin{aligned} A_{1,L_i}^b &= \gamma_1 A_{1,1}^b, A_{2,L_i}^b = \gamma_2 IV_{2,1}^b, \\ A_{3,L_i}^b &= \gamma_3 IV_{3,1}^b, V_J^b = \gamma_V V_1^b \end{aligned} \tag{15}$$

Step 3: Determine other input and output reference values in BRB_b.

Step 1 actually describes the distribution or relationship of the input and output reference values in their respective variation ranges in BRB_a. After the variation range of $f_1^b(t), f_2^b(t), f_3^b(t)$ and $y^b(t+n)$ are fixed in step 2, the interval width $D_{b,i}$ and $D_{b,4}$ of the input and output reference values in BRB_a can be obtained by Eq. (12). Then, the distribution of BRB_a can be transferred to BRB_b to obtain other reference values by Eq. (16). Obviously, after transferring operation, the number of input and output reference values in BRB_b and BRB_a are same, the number of rules is same as well, and the belief distribution of the consequent attribute in each rule in both models are set as the same.

$$A_{i,\tau}^b = D_{b,i}\mu_{i,\tau} + A_{i,1}^b, V_\lambda^b = D_{b,4}\varphi_\lambda + V_1^b \tag{16}$$

4.2. SLP-based Online Optimization of Belief Parameters of the Consequent Attribute of Belief Rule

The obtained BRB_b model is a relatively rough model, because $\beta_{k,j}^b$, which is the belief degree of the consequent attribute, is directed copied from BRB_a. Thus, it cannot accurately describe the situation that the output changes with the input. Essentially, BRB_b model adopts the current input $f_1^b(t), f_2^b(t), f_3^b(t)$ at time t to predict the sliding force of future $f^b(t+n)$ at time $t+n$, with the predicted sliding force set as $y^b(t+n)$. Obviously, optimization aims to minimize the difference between $f^b(t+n)$ and $y^b(t+n)$, thus the objective function based on minimum mean squared error is set as shown in Eq. (17).

$$\begin{aligned} &\min_P \xi(P) \\ &\xi(P) = \sum_{q=1}^{Q} \frac{1}{Q}\left(f^b(q) - y^b(q)\right)^2 \end{aligned} \tag{17}$$

where $P = \left\{\beta_{k,j}^b(t) | k = 1, 2, ..., K^b, j = 1, 2, ..., J\right\}$ is a parameter set which needs to be optimized, and it consists of the belief degrees of the consequent attribute of the activated rule in BRB_b at time t. K^b stands for the number of the activated rules at time t, which must satisfy the constrains shown in Eq. (18).

$$0 \le \beta_{k,j}^b(t) \le 1, \sum_{j=1}^{J} \beta_{k,j}^b(t) = 1 \tag{18}$$

And the Q historical data samples of the monitoring point *No.2* which are obtained online can be adopted to do optimization. For example, if $n = 2$, the historical data samples $\left(f_1^b(t-3), f_2^b(t-3), f_3^b(t-3), f^b(t-1)\right)$, $\left(f_1^b(t-4), f_2^b(t-4), f_3^b(t-4), f^b(t-2)\right)$ which are obtained at time $t-1$ and $t-2$ can be used to optimize $\beta_{k,j}^b(t)$ at time t with $Q=2$.

SLP is adopted to solve online optimization problems. To be specific, the optimal belief degrees obtained at time t will be used as the initial values of the belief degrees at time $t+1$. And the online optimization process is achieved iteratively in a similar fashion. The basic principle of SLP is that the first-order Taylor series expansion of the nonlinear function is adopted so as to approximately convert the nonlinear problem to a series of linear programming problems. And SLP can simply construct the first-order Taylor expansion of the linear approximation model through analytical methods or finite difference methods, so as to avoid the calculation of complex higher order derivatives [27]. To be specific, the iterative optimization process based on SLP includes the following four steps:

Step 1: Calculate the first-order partial derivative of the nonlinear optimization objective function.

Based on the parameter optimization model in Eq. (17), the first-order partial derivative of the objective function $\xi(P)$ is calculated, and the linear transformation as shown in Eq. (19) is implemented, where P_0 represents a given initial point. Then, the nonlinear optimization problem $\min_P \xi(P)$ is transformed into a linear programming problem $\min_P \xi'\left(P_0\right)P$.

$$\xi(P) \approx \xi\left(P_0\right) + \xi'\left(P_0\right)\left(P - P_0\right) \tag{19}$$

Step 2: Determine the moving limits of the optimized parameters.

The selection of moving limits directly affects the effectiveness of the SLP optimization algorithm. Specifically, large moving limits will reduce accuracy, while small moving limits lead to the increment of the number of iterations and calculation thereby extending of the program running time. Here, the upper bound of the parameters to be optimized is shown in Eq. (20). Normally, the moving limits are set less than or equal to 10% of this upper bound, which is less than or equal to 0.1.

$$UB\left(\beta_{k,j}^b\right) = 1, k = 1, 2, \ldots, K^b, j = 1, 2, \ldots, J \tag{20}$$

Step 3: Use linear programming to obtain local optimal value.

A search space is established by setting the initial points and moving limits. And a linear programming method, e.g., an interior point method, is used to complete the search process [28, 29]. Specifically, if the intersection of the search space and the linearized feasible solution space is empty, the search space needs to be expanded by increasing the moving limits. If there is an intersection, the optimal solution of the linear programming problem will be searched in intersection [30]. Next, take the obtained optimal solution as a new initial point, re-linearize the original nonlinear optimization objective function, and iteratively execute the entire process until the given stopping criterion is achieved.

Step 4: Stop criterion.

When 1) the moving limits of all parameters are reduced to a significantly small value, or 2) the value of the parameters or the value of the objective function does not change significantly during two iterations, the SLP iteration process should be stopped.

5. EXPERIMENTS AND ANALYSIS OF SLIDING FORCE PREDICTION

5.1. Construct BRB$_a$ Based on Historical Data of Monitoring Point No.1

BRB$_a$ is constructed by the sliding force of the rising stage (Section BC) at the monitoring point *No.1* in Figure 3. Concretely, the sampling time corresponding to B is 3 o'clock on February 22, 2008 and the sliding force increases from a relatively stable 278.5 kN to 294.08 kN at this point, where kN is an international unit for measuring the size of the force. The sampling time corresponding to C is 9 o'clock on March 15, 2008, the sliding force drops from the largest 588.95 kN to 296.02 kN at this point, which indicates that the structure of the slope body has changed at this moment. All in all, it takes 486 hours from the abnormal increase of the sliding force at B to the change of the slope body structure at C, and 178 sets of measurement data are collected.

5.1.1. Determine input and output reference values in BRB$_a$

Regarding to the 178 sets of data, a dataset $\left\{\left(f_1(t), f_2(t), f_3(t), y(t+2)\right) | t = 3, 4, \ldots, 181\right\}$ can be constructed from Eq. (3). And $n = 2$ is taken as an example to introduce the entire modeling process, that is, the constructed BRB model can be two sampling cycles (6 hours) in advance to obtain the predicted value $y(t+2)$ of $f(t+2)$. Then, contained by the limitation of the computer hardware, K = 4 is chosen to cluster the variables, which can not only have enough reference values, but also reduce the complexity of the experiment. And there are 6 reference values of input variables $f_1(t), f_2(t), f_3(t)$ and output variable $y(t+2)$ respectively, which are described by fuzzy semantic values as: very small *VS*, positive small *PS*, median *PM*, positive large *PL*, medium large *ML*, very large *VL*. The reference values of the input and output variables are shown in Table 3.

5.1.2. Obtain belief rules in BRB$_a$

Based on the reference values provided in Table 3, BRB$_a$ can be constructed, and the k-th rule is expressed as Eq. (21), where $A_{k,1}$, $A_{k,2}$ and $A_{k,3}$, respectively, stand for any of the corresponding reference values in Table 3.

$$\begin{aligned} R_k:\ & \text{If } \left(f_1(t) \text{ is } A_{k,1}\right) \wedge \left(f_2(t) \text{ is } A_{k,2}\right) \wedge \left(f_3(t) \text{ is } A_{k,3}\right) \\ & \text{Then } y(t+2) \text{ is } \left\{\left(V_1, \beta_{k,1}\right), \left(V_2, \beta_{k,2}\right), \ldots, \left(V_6, \beta_{k,6}\right)\right\}, \\ & \sum_{j=1}^{6} \beta_{k,j} = 1, k \in \{1, 2, \ldots, 216\} \end{aligned} \tag{21}$$

Table 3 The reference value (semantic value) of input and output variables in BRB_a.

Input variable $f_1(t)$	**Semantic value**	$A_{1,1}(VS)$	$A_{1,2}(PS)$	$A_{1,3}(PM)$	$A_{1,4}(PL)$	$A_{1,5}(ML)$	$A_{1,6}(VL)$
	Reference value	295.0855	320.3768	382.6278	460.0012	549.9463	585.5067
Input variable $f_2(t)$	**Semantic value**	$A_{2,1}(VS)$	$A_{2,2}(PS)$	$A_{2,3}(PM)$	$A_{2,4}(PL)$	$A_{2,5}(ML)$	$A_{2,6}(VL)$
	Reference value	−0.2140	0.7225	1.5206	3.0613	3.4339	10.4008
Input variable $f_3(t)$	**Semantic value**	$A_{3,1}(VS)$	$A_{3,2}(PS)$	$A_{3,3}(PM)$	$A_{3,4}(PL)$	$A_{3,5}(ML)$	$A_{3,6}(VL)$
	Reference value	0.0000	0.7209	1.5265	3.0571	3.4091	6.8430
Output variable $y(t+2)$	**Semantic value**	$V_1(VS)$	$V_2(PS)$	$V_3(PM)$	$V_4(PL)$	$V_5(ML)$	$V_6(VL)$
	Reference value	295.8567	321.8439	385.7263	466.7651	559.0389	587.9533

Table 4 Part of rules in BRB_a.

k	The Combination of Antecedent Reference Values	The Consequent Belief Distribution					
		β_1	β_2	β_3	β_4	β_5	β_6
1	$VS \wedge VS \wedge VS$	0.9209	0.0791	0	0	0	0
2	$VS \wedge VS \wedge PS$	0.9407	0.0593	0	0	0	0
3	$VS \wedge VS \wedge PM$	0.9407	0.0593	0	0	0	0
4	$VS \wedge VS \wedge PL$	0.9407	0.0593	0	0	0	0
5	$VS \wedge VS \wedge ML$	0.9407	0.0593	0	0	0	0
⋮	⋮	⋮	⋮	⋮	⋮	⋮	⋮
96	$VS \wedge PL \wedge VL$	0	0	0.9724	0.0276	0	0
97	$VS \wedge ML \wedge VS$	0	0	0.9599	0.0401	0	0
98	$VS \wedge ML \wedge PS$	0	0.0285	0.9715	0	0	0
99	$PM \wedge ML \wedge PM$	0	0.0285	0.9715	0	0	0
⋮	⋮	⋮	⋮	⋮	⋮	⋮	⋮
137	$PL \wedge ML \wedge ML$	0	0	0.013	0.987	0	0
138	$PL \wedge ML \wedge VL$	0	0	0.013	0.987	0	0
139	$PL \wedge VL \wedge VS$	0	0	0	0.9446	0.0554	0
140	$PL \wedge VL \wedge PS$	0	0	0	0.9446	0.0554	0
⋮	⋮	⋮	⋮	⋮	⋮	⋮	⋮
212	$VL \wedge VL \wedge PS$	0	0	0	0	0	1
213	$VL \wedge VL \wedge PM$	0	0	0	0	0	1
214	$VL \wedge VL \wedge PL$	0	0	0	0	0.192	0.808
215	$VL \wedge VL \wedge ML$	0	0	0	0	0.192	0.808
216	$VL \wedge VL \wedge VL$	0	0	0	0	0.192	0.808

And the weight of the rule θ_k and the attribute weight δ_i are both set as 1, which means that 216 rules have equal belief degree and the input variables have the same importance in determining the output variables. By matching the historical input variable with the reference vector in the k-th rule according to Eq. (4) in Section 3.3, the most similar historical data samples are found, so as to calculate the belief degrees of the consequent attribute in the k-th rule $\beta_{k,1}, \ldots, \beta_{k,6}$ by Eq. (5). Table 4 lists part of rules of BRB_a.

5.1.3. Obtain predicted sliding force based on ER algorithm

After the input variables $\left(f_1(t), f_2(t), f_3(t)\right)$ are obtained online, Eq. (6) is adopted to calculate the activated rule weights. Then the ER algorithm, as shown in Eqs. (10) and (11), is adopted to obtain the fused belief distribution as shown in Eq. (9). Finally, the predicted value $y(t+2)$ can be acquired by weighting the output reference value.

Take data samples $\left(f_1(t), f_2(t), f_3(t)\right) = (295.5996, 0.5141, 1.0283)$ obtained at $t = 4$ as an example, it illustrates how to obtain the prediction $y(t+2)$ by fusion reasoning. Calculating from Eq. (5), the matching degree of $f_1(t) = 295.5996$ with the reference values VS and PS in Table 3 are 0.9797 and 0.0203, the matching degree of $f_2(t) = 0.5141$ with the reference values VS and PS are 0.2225 and 0.7775, the matching degree of $f_3(t) = 1.0283$ with PS and PM are 0.6184 and 0.3816, and the matching degree with the other reference values are 0.

According to the reference value activated by each variable, there are 8 activated rules R_2, R_3, R_8, R_9, R_{38}, R_{39}, R_{44}, R_{45}. And Eq. (6) is adopted to calculate the corresponding activated weights such as $w_2 = 0.1348$, $w_3 = 0.0832$, $w_8 = 0.471$, $w_9 = 0.2906$, $w_{38} = 0.0028$, $w_{39} = 0.0017$, $w_{44} = 0.0098$, $w_{45} = 0.006$. The fused belief distribution obtained by ER algorithm is $\{(V_1, 0.9491), (V_2, 0.0509), (V_3, 0), (V_4, 0), (V_5, 0), (V_6, 0)\}$. And the predicted value $y(t+2) = 297.1794$, whose corresponding true value is $f_1(t+2) = 297.3987$, can be achieved by weight sum of the belief degree of the reference

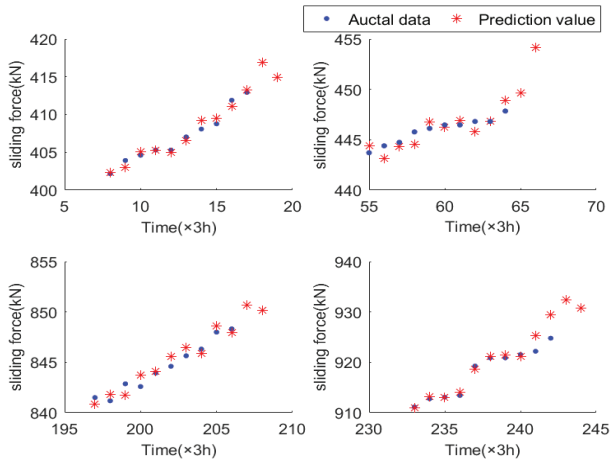

Figure 5 The predicted value of sliding force in BRB_a.

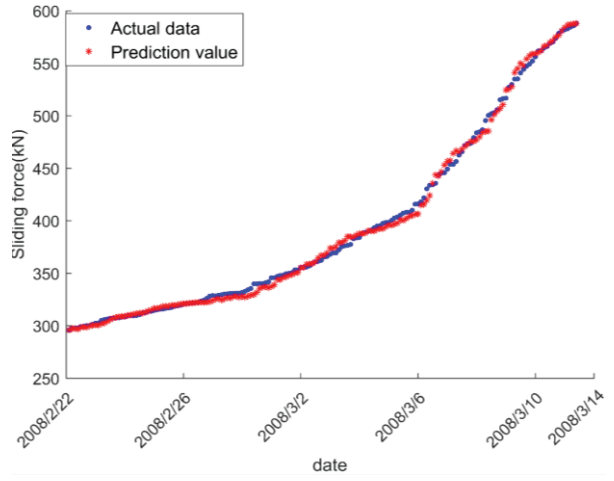

Figure 6 The sliding force prediction of all samples in BRB_a.

values. Obviously, it can be seen that the model provides accurate prediction results.

For all the remaining input variables, the corresponding predicted output values can be obtained through the above-reasoning process. As shown in Figure 5, the actual data and the predicted values at $t = 18, 43, 110, 172$ are given, respectively. And the predicted values of all data samples are given in Figure 6. Finally, the mean absolute percentage error (MAPE) of all samples equals to 0.008. To conclude, the established BRB_a based on historical data can accurately predict the sliding force at time $t + 2$.

5.2. Model Transfer from BRB_a to BRB_b

Seen from Figure 4, the sliding force at the monitoring point *No.2* was observed from 0:00 on January 1, 2008, and real-time overrun detection was performed. When the increase of sliding force between two samplings exceeds 10 kN, the model transfer which is illustrated in Section 4.1 is implemented from BRB_a to BRB_b. For example, at sampling time B' in Figure 4 (6:00 on February 11, 2008), the sliding force increased from 376.5 kN to 398.3655 kN, thus the change amount is over 10 kN. At this moment, the model transfer needs to be implemented.

5.2.1. Parameter transfer of BRB_b model

Firstly, the interval width of the reference values in BRB_a is calculated by Eq. (12). To be specific, the interval width of the input reference values is $D_{a,1} = 289.4212$, $D_{a,2} = 10.6148$, $D_{a,3} = 6.843$ and the interval width of the output reference value is $D_{a,4} = 292.0786$. Then the relative position ratio of the number of clustering centers of input and output variables in BRB_a can be calculated by Eq. (13), which are $\mu_{1,2} = 0.0874$, $\mu_{1,3} = 0.3025$, $\mu_{1,4} = 0.5698$, $\mu_{1,5} = 0.8806$, $\mu_{2,2} = 0.0882$, $\mu_{2,3} = 0.1634$, $\mu_{2,4} = 0.3086$, $\mu_{2,5} = 0.3437$, $\mu_{3,2} = 0.1054$, $\mu_{3,3} = 0.2231$, $\mu_{3,4} = 0.4468$, $\mu_{3,5} = 0.4982$, $\varphi_2 = 0.089$, $\varphi_3 = 0.3077$, $\varphi_4 = 0.5851$, $\varphi_5 = 0.8908$.

Set the time at B' as $t = 1$ with $f_1^b(1) = 398.3655$, then the minimum value of the input reference values $f_1^b(t)$ and the output reference value $y^b(t+n)$ in the BRB_b model are set as $A_{1,1}^b = V_1^b = 398.3655$. By continuing to sampling, $f_1^b(2) = 399.0595$ and $f_1^b(3) = 399.4065$ can be obtained, and the initial value of $f_2^b(3) = 0.347$ and $f_3^b(3) = 0.5205$ can be obtained from Eq. (3), with $IV_{2,1}^b = 0.347$, $IV_{3,1}^b = 0.5205$. The reduction factors $\sigma_1 = -3$ and $\sigma_2 = -1$ are determined by experts, and the minimum reference value of the two input variables $A_{2,1}^b = -1.041$ and $A_{3,1}^b = -0.5205$ can be calculated from Eq. (14). And the maximum reference values $A_{1,6}^b = 995.9137$, $A_{2,6}^b = 17.35$, $A_{3,6}^b = 10.4102$, $V_6^b = 995.9137$ can be calculated from Eq. (15), with the experts determined enlargement factors are set as $\gamma_1 = 2.5, \gamma_2 = 50, \gamma_3 = 20$ and $\gamma_V = 2.5$. Finally, the interval width of the input and output reference values in BRB_b can be obtained by $D_{b,1} = 597.5482$, $D_{b,2} = 18.391$, $D_{b,3} = 10.9307$ and $D_{b,4} = 597.5482$ from Eq. (12), and the other reference values of input and output variables in $BRB_b$are calculated by Eq. (16). And all model parameters after transferring are shown in Table 5.

5.2.2. Online iterative optimization of belief degree parameters in BRB_b based on SLP

The initial BRB_b model can be generated by the parameter transfer described in Section 5.2.1. In the initial BRB_b model, the number of rules and the belief distribution of the consequent attributes in each rule are consistent with BRB_a as shown in Table 4, except that the reference value of antecedent attributes are replaced with BRB_b as shown in Table 5. In this experiment, BRB_b model makes prediction of two steps in advance ($n = 2$), thus at time $t = 3, 4, 5$ there are no historical data samples can be used for online optimization in BRB_b, then the output is determined by the initial BRB_b. Table 6 shows the predicted values $y^b(t+n)$ and its corresponding true values $f^b(t+n)$ of the three time. It can be seen that the predicted results are close to the true values, which indicates that the BRB_b obtained after the parameter transfer is able to predict the sliding force at monitoring point *No.2*.

In order to increase the prediction accuracy of BRB_b at subsequent times, when at $t = 7$, historical data samples $\left(f_1^b(4), f_2^b(4), f_3^b(4), f_1^b(6)\right) = (401.4882, 2.0817, 1.2143, 403.9196)$ at $t = 4$ are selected to optimize the belief parameters of the initial BRB_b by the method which is described in Section 4.2.

Table 5 Reference value (semantic value) of input and output variables in BRB_b.

Input variable $f_1(t)$	**Semantic value**	$\boldsymbol{A^b_{1,1}(VS)}$	$\boldsymbol{A^b_{1,2}(PS)}$	$\boldsymbol{A^b_{1,3}(PM)}$	$\boldsymbol{A^b_{1,4}(PL)}$	$\boldsymbol{A^b_{1,5}(ML)}$	$\boldsymbol{A^b_{1,6}(VL)}$
	Reference value	**398.3655**	**450.5825**	**579.1081**	**738.8556**	**924.5593**	**995.9137**
Input variable $f_2(t)$	**Semantic value**	$\boldsymbol{A^b_{2,1}(VS)}$	$A^b_{2,2}(PS)$	$A^b_{2,3}(PM)$	$A^b_{2,4}(PL)$	$A^b_{2,5}(ML)$	$A^b_{2,6}(VL)$
	Reference value	−1.0410	1.9696	3.3524	6.0217	6.6673	17.3500
Input variable $f_3(t)$	**Semantic value**	$A^b_{3,1}(VS)$	$A^b_{3,2}(PS)$	$A^b_{3,3}(PM)$	$A^b_{3,4}(PL)$	$A^b_{3,5}(ML)$	$A^b_{3,6}(VL)$
	Reference value	−0.5205	1.6721	2.9590	5.4038	5.9660	10.4102
Output variable $y(t+2)$	**Semantic value**	$\boldsymbol{V^b_1(VS)}$	$\boldsymbol{V^b_2(PS)}$	$\boldsymbol{V^b_3(PM)}$	$\boldsymbol{V^b_4(PL)}$	$\boldsymbol{V^b_5(ML)}$	$\boldsymbol{V^b_6(VL)}$
	Reference value	398.3655	451.5314	582.2250	748.0180	930.6586	995.9137

Table 6 Input variables and output variables at three moments in BRB_b.

t	$f_1^b(t)$	$f_2^b(t)$	$f_3^b(t)$	$y^b(t+n)$	$f^b(t+n)$
3	399.4065	0.347	0.5205	402.1133	402.182
4	401.4882	2.0817	1.2143	404.0322	403.9196
5	402.182	0.6938	1.3877	403.5488	404.6097

Table 7 The optimized rule at t = 7 in $BRB_b{}^o(7)$.

k	The Combination of Antecedent Reference Values	The Consequent Belief Distribution					
		β_1^b	β_2^b	β_3^b	β_4^b	β_5^b	β_6^b
1	$VS \wedge VS \wedge VS$	0.9209	0.0791	2.51e-15	8.83e-16	5.13e-16	4.26e-16
2	$VS \wedge VS \wedge PS$	0.9407	0.0593	3.26e-15	1.15e-15	6.67e-16	5.79e-16
7	$VS \wedge PS \wedge VS$	0.9209	0.0791	8.28e-16	2.91e-16	1.69e-16	1.47e-16
8	$VS \wedge PS \wedge PS$	0.9407	0.0593	1.17e-15	4.1e-16	2.37e-16	2.06e-16
37	$PS \wedge VS \wedge VS$	0.0044	0.9956	1.7e-14	1.69e-14	1.09e-14	9.79e-15
38	$PS \wedge VS \wedge PS$	0.0142	0.9858	5.0e-14	2.31e-14	1.43e-14	1.27e-14
43	$PS \wedge PS \wedge VS$	0.0241	0.9759	1.62e-14	8.38e-15	5.47e-15	4.86e-15
44	$PS \wedge PS \wedge PS$	0.0241	0.0759	2.0e-14	1.04e-14	6.81e-15	6.05e-15

Specifically, when $\left(f_1{}^b(4), f_2{}^b(4), f_3{}^b(4)\right)$ are imported into the initial BRB_b model, 8 rules will be activated which are R_1, R_2, R_7, R_8, R_{37}, R_{38}, R_{43}, R_{44}, then the belief degrees need to be optimized is $P(t=4) = \left\{\beta_{k,j}^b | k = 1, 2, 7, 8, 37, 38, 43, 44; j = 1, 2, \ldots, 6\right\}$. Set the rule weight and attribute weight as 1, the minimum interval increment as 4e-05, the optimization stop error as 1e-06, respectively. And, then the objective function shown in Eq. (16) and the SLP online optimization steps shown in Section 4.2 are adopted to optimize the belief degrees of the activated rules. At this time, in order to reduce the duration of the iterative optimization, only one historical sample is used to optimize the parameters, so $Q = 1$ in Eq. (16). Table 7 demonstrates the results of local optimization, with the optimized BRB denoted as $BRB_b^o(7)$, and the superscript "o" stands for "optimization." Then, the predicted value of inputting $\left(f_1^b(4), f_2^b(4), f_3^b(4)\right)$ into $BRB_b^o(7)$ is $y^b(7) = 406.2815$.

When $t = 8$, there is the initial BRB $BRB_b(8) = BRB_b^o(7)$. And the SLP online optimization steps are repeated based on the historical data samples $\left(f_1^b(5), f_2^b(5), f_3^b(5), f_1^b(7)\right)$ to obtain the optimized $BRB_b^o(8)$ before $t = 9$, and further obtain the predicted value $y^b(8) = 405.3485$. Similarly, at time t, optimization before prediction forms the entire iterative optimization and inference prediction process. Table 8 shows the BRB at the time of prediction termination at $C'(t = 247)$ in Figure 4. Comparing with the initial BRB at $t = 1$ shown in Table 4, it unveils that the belief degrees of all consequent attributes have been updated. Figure 7 shows the true and predicted values obtained after dynamic optimization and inference at $t = 17, 64, 206, 242$, respectively. And the comparison of the predicted value of iteratively optimized $BRB_b{}^o$, the initial BRB_b obtained without optimization and true values of all samples are shown in Figure 8. Finally, the mean absolute percentage error of the former is MAPE = 0.0061 and the mean absolute percentage error of the latter is MAPE = 0.0108. It can be seen that the iterative optimization process significantly improves the overall accuracy of prediction. Obviously, seen from the figure, the early rise of the sliding force is relatively smooth ($t = 1 \sim 80$), and the prediction of the sliding force iterative optimization is accurate. But, when the rise goes steeper ($t = 119 \sim 131$), a certain deviation will occur because the change laws of input and output have changed obviously. When the model parameters are continuously updated iteratively, the transferred new BRB will be more suitable for the change law of the real data.

Table 8 The optimized belief rule base.

k	The Combination of Antecedent Reference Values	The Consequent Belief Distribution					
		β_1^b	β_1^b	β_1^b	β_1^b	β_1^b	β_1^b
1	$VS \wedge VS \wedge VS$	0.9863	7.29e-13	9.49e-13	1.88e-12	4.57e-07	0.0133
2	$VS \wedge VS \wedge PS$	0.9835	1.27e-13	2.83e-13	1.41e-12	1.14e-07	0.0165
3	$VS \wedge VS \wedge PM$	0.9455	0.0392	5.77e-10	1.14e-08	0.0076	0.0076
4	$VS \wedge VS \wedge PL$	0.9407	0.0593	0	0	0	0
5	$VS \wedge VS \wedge ML$	0.9407	0.0593	0	0	0	0
⋮	⋮	⋮	⋮	⋮	⋮	⋮	⋮
96	$VS \wedge PL \wedge VL$	0.0365	0.0108	0.861	0.0306	0.0306	0.0306
97	$VS \wedge ML \wedge VS$	0	0	0.9599	0.0401	0	0
98	$VS \wedge ML \wedge PS$	0	0.0285	0.9715	0	0	0
99	$PM \wedge ML \wedge PM$	0.0685	0.0277	0.837	0.0223	0.0223	0.0223
⋮	⋮	⋮	⋮	⋮	⋮	⋮	⋮
134	$PL \wedge ML \wedge MS$	0	0	0.013	0.987	0	0
135	$PL \wedge ML \wedge PM$	0.0487	0.0196	0.0136	0.9008	0.0086	0.0086
136	$PL \wedge ML \wedge PL$	0.0264	0.0264	0.0191	0.8577	0.0423	0.0282
137	$PL \wedge ML \wedge ML$	0.0112	0.0112	0.0112	0.8316	0.0781	0.0567
⋮	⋮	⋮	⋮	⋮	⋮	⋮	⋮
212	$VL \wedge VL \wedge PS$	0	0	0	0	0	1
213	$VL \wedge VL \wedge PM$	0	0	0	0	0	1
214	$VL \wedge VL \wedge PL$	0.0017	0.0017	9.52e-10	2.91e-11	0.1403	0.8563
215	$VL \wedge VL \wedge ML$	0.0017	0.0017	1.36e-10	8.02e-12	0.0953	0.9012
216	$VL \wedge VL \wedge VL$	0.0051	0.0051	7.96e-10	2.68e-08	0.1369	0.8529

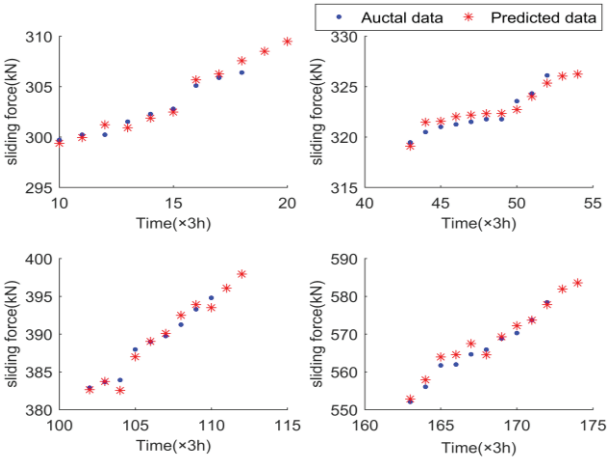

Figure 7 The sliding force prediction at part of time in BRB_b^o.

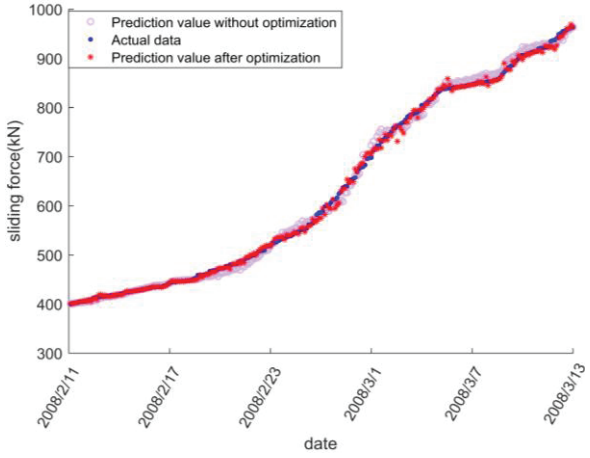

Figure 8 The comparison of prediction in initial BRB_b and the iterative optimization BRB_b^o.

5.3. Expansion Test Experiment and Analysis

In order to verify the effectiveness of the proposed model transfer and parameter online optimization methods, linear disturbances and sinusoidal function disturbances are implemented on the sliding force data at monitoring point *No.2*, which changes the overall or local variation trends of the sliding force. As shown in the Figure 9, the upper picture shows the case of adding linear disturbance which increases the sliding force changing rate and expands the sliding force range. And the under picture demonstrates the situation of adding nonlinear disturbance which makes the local trend of the sliding force more uncertain. Model transfer and parameter optimization are implemented based on BRB_a so that a new BRB is generated for sliding force prediction. The simulation results in Figure 9 prove that the proposed method has good robustness, and relatively accurate prediction results are given in both cases.

6. SUMMARY

To tackle the uncertain problem which is caused by variation of sliding force, a method of slope sliding force prediction based on BRB inferential methodology is proposed in the paper to achieve accurate prediction of different slope sliding force measurement points. The main contributions of this paper are demonstrated as follows:

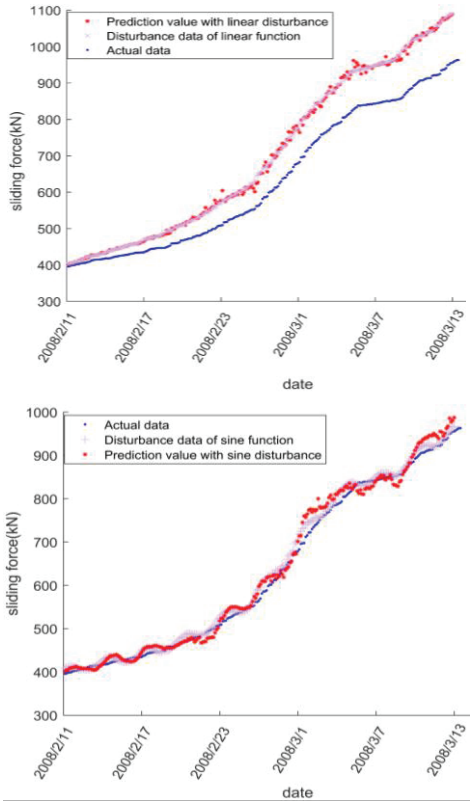

Figure 9 The predictions of adding different disturbances to the sliding force at monitoring point *No.2*.

(1) BRB prediction model based on historical data is established. A BRB prediction model is constructed so as to describe the nonlinear mapping relationship between input (history, current sliding force) and output (future sliding force). ER algorithm is adopted to fuse the belief rules which are activated by input. Based on the fused results, the prediction of the sliding force can be calculated.

(2) A parameter transfer of the BRB sliding force prediction model for new monitoring points is proposed. Based on historical data, the BRB and the relative position ratio of the input and output reference values are determined. By transference and transformation of the determined values, the BRB and the input and output reference values of the sliding force prediction model at new monitoring points can be obtained.

(3) Local iteration optimization of model parameters strategy is adopted. For the adaptive adjustment of BRB models at different monitoring points, SLP is used to iteratively optimize and update the parameters activated in the BRB model after transference, so as to improve the prediction accuracy of the model.

In addition, there are still some worthy problems for further discussion and research:

(1) As the factors which influencing the slope stability are complicated, such as groundwater, fracture, ground stress, and directly obtaining the data by NPR anchor cable has some limitations, the prediction and stability analysis of slope sliding with a variety of uncertain information needs further study.

(2) In this paper, the measurement samples of the NPR anchor cable are complete. However, the measurement data is incomplete in reality. In future studies, it is worth further discussing and extending this aspect.

(3) When the sliding force is abrupt, the internal structure of the slope changes, and the prediction model cannot be used. How to solve the abrupt sliding force prediction needs further study.

CONFLICTS OF INTEREST

We confirm that the manuscript has been read and approved by all named authors and that there are no other persons who satisfied the criteria for authorship but are not listed. We further confirm that the order of authors listed in the manuscript has been approved by all of us.

AUTHORS' CONTRIBUTIONS

Jing Feng: conceived of the presented idea and wrote the manuscript. Xiaobin Xu: developed the theory. Pan Liu: carried out the experiment. Feng Ma: performed the calculations. Chengrong Ma: contributed to the interpretation of the results. Zhigang Tao: contributed to data preparation and analysis. All authors provided critical feedback and helped shape the research, analysis and manuscript.

ACKNOWLEDGMENTS

This work was supported by the Zhejiang Province Key R&D projects (No.2019C03104), the NSFC-Zhejiang Joint Fund for the Integration of Industrialization and Informatization (No.U1709215), the Zhejiang Provincial Basic Public Welfare Research Project (No. LGF21F020013), the Open Research Project of the State Key Laboratory of Industrial Control Technology, Zhejiang University, China (No. ICT20028), the Second Tibetan Plateau Scientific Expedition and Research Program (No. 2019QZKK0707), the NSFC (No. 61751304).

REFERENCES

[1] I. Vujadin, B. Ivan, Application of LiDAR technology in analyses of the topography of Margum/Morava and Kuli, Starinar. 62 (2012), 239–255.
[2] Y. Sun, H. Xu, P. Gu, W. Hu, Application of FBG sensing technology in stability analysis of geogrid-reinforced slope, Sensors (Basel, Switzerland). 17 (2017), 597.
[3] X. Zhao, Y. Sun, Q. Feng, Analysis on the influence of heavy rainfall on slope stability, IOP Conf. Ser. Earth Environ. Sci. 170 (2018), 022010.
[4] P. Ni, G. Mei, Y. Zhao, Influence of raised groundwater level on the stability of unsaturated soil slopes, Int. J. Geomech. 18 (2018), 04018168.

[5] R. Makharoblidze, I. Lagvilava, B. Basilashvili, R. Khazhomia, Influence of slip on lateral displacement of the tractor on slope, Ann. Agrar. Sci. 15 (2017), 201–203.
[6] J. Feng, Z. Tao, D. Li, Evaluation of slope stability by the in situ monitoring data combined with the finite-discrete element method, Procedia Eng. 191 (2017), 568–574.
[7] M. He, X. Han, B. Zhang, Z. Tao, Real-time remote monitoring and forecasting technology for landslide disasters based on sliding force variation and its engineering application, J. Heilongjiang Univ. Sci. Technol. 22 (2012), 337–342. https://kns.cnki.net/kcms/detail/detail.aspx?FileName=HLJI201204005&DbName=CJFQ2012
[8] Z. Tao, H. Xu, C. Zhu, The study of the supernormal mechanical properties of giant NPR anchor cables, Shock Vib. 2020 (2020), 1–13.
[9] X. Sun, B. Zhang, L. Gan, Z. Tao, C. Zhao, Application of constant resistance and large deformation anchor cable in soft rock highway tunnel, Adv. Civil Eng. 2019 (2019), 1–19.
[10] R. Bai, P. Zhang, J. Liu, The artificial neural network model of forecasting open mining slope stability, J. Liaoning Tech. Univ. Nat. Sci. 19 (2000), 337–339. https://kns.cnki.net/kcms/detail/detail.aspx?FileName=MCXB200002005&DbName=CJFQ2000
[11] X. Li, J. Kong, J. Xie, Support vector machine method for stability prediction of rock slopes in hydropower engineering regions, J. Coal Sci. Eng. 36 (2011), 259–263.
[12] L. Wang, Q. Zhang, W. Liu, The application of kalman filter based GM model in road slop deformation monitoring, Geotech. Invest. Surv. 2007 (2007), 56–59. https://kns.cnki.net/kcms/detail/detail.aspx?FileName=GCKC200703012&DbName=CJFQ2007
[13] G. Sun, Z. Tao, J. Yang, *et al.*, Monitoring and early-warning of fault landslide in Pingzhuang west open-cast coal mine, Metal Mine. 45 (2016), 51–55. https://kns.cnki.net/kcms/detail/detail.aspx?FileName=JSKS201602011&DbName=CJFQ2016
[14] Z. Tao, X. M, C. Meng, *et al.*, Analysis of wedge-shaped landslide mechanism and sliding force monitoring warning in Nanfen open pit iron mine, J. China Coal Soc. 42 (2017), 3149–3158.
[15] S. Zhang, X. Zhang, X. Pei, S. Wang, R. Huang, Q. Xu, Model test study on the hydrological mechanisms and early warning thresholds for loess fill slope failure induced by rainfall, Eng Geol. 258 (2019), 105135.
[16] Z. Tao, C. Zhu, X. Zheng, Slope stability evaluation and monitoring of Tonglushan ancient copper mine relics, Adv. Mech. Eng. 10 (2018), 1–16.
[17] X. Xu, Z. Liu, Y. Chen, Circuit tolerance design using belief rule base, Math. Probl. Eng. 2015 (2015), 1–12.
[18] L. Yang, Y. Wang, Y. Lan, L. Chen, Y. Fu, A Data Envelopment Analysis (DEA)-based method for rule reduction in extended belief-rule-based systems, Knowl. Based Syst. 123 (2017), 174–187.
[19] L. Yang, Y. Wang, J. Liu, L. Martínez, A joint optimization method on parameter and structure for belief-rule-based systems, Knowl. Based Syst. 142 (2018), 220–240.
[20] L. Yang, Y. Wang, Q. Su, Y. Fu, K. Chin, Multi-attribute search framework for optimizing extended belief rule-based systems, Inf. Sci. 370–371 (2016), 159–183.
[21] L. Chang, W. Dong, J. Yang, X. Sun, X. Xu, X.J. Xu, L. Zhang, Hybrid belief rule base for regional railway safety assessment with data and knowledge under uncertainty, Inf. Sci. 518 (2012), 376–395.
[22] X. Xu, Z. Zhao, X. Xu, J. Yang, L. Chang, X. Yan, G. Wang, Machine learning-based wear fault diagnosis for marine diesel engine by fusing multiple data-driven models, Knowl. Based Syst. 190 (2020), 105324.
[23] L. Chang, J. Jiang, J. Sun, Chen, Y. Zhou, Z.J. Xu, X. Xu, Disjunctive belief rule base spreading for threat level assessment with heterogeneous, insufficient and missing information, Inf. Sci. 476 (2018), 106–131.
[24] X. Xu, Z. Li, G. Li, An acoustic resonance-based liquid level detector with error compensation, IEEE Trans. Instrum. Meas. 68 (2019), 963–971.
[25] X. Xu, H. Xu, C. Wen, J. Li, P. Hou, J. Zhang, A belief rule-based evidence updating method for industrial alarm system design, Control Eng. Pract. 81 (2018), 73–84.
[26] L. Chang, Z. Zhou, Y. Chen, X. Xu, J.B. Sun, T. Liao, X. Tan, Akaike information criterion-based conjunctive belief rule base learning for complex system modeling, Knowl. Based Syst. 161 (2018), 47–64.
[27] Z. Drezner, P. Kalczynski, Solving nonconvex nonlinear programs with reverse convex constraints by sequential linear programming, Int. Trans. Oper. Res. 27 (2020), 1320–1342.
[28] M. Vaccari, G. Mancuso, J. Riccardi, M. Cantù, G. Pannocchia, A sequential linear programming algorithm for economic optimization of hybrid renewable energy systems, J. Process Control. 74 (2019), 189–201.
[29] M. Willis, V. von Stosch, L0-constrained regression using mixed integer linear programming, Chemom. Intell. Lab. Syst. 165 (2017), 29–37.
[30] Y. Ma, Q. Cai, S.Y. Yao, Integer linear programming models for the weighted total domination problem, Appl. Math. Comput. 358 (2019), 146–150.